Cryogenics 50 (2010) 743–749

Contents lists available at ScienceDirect

Cryogenics

journal homepage: www.elsevier.com/locate/cryogenics

CFD analysis of thermodynamic cycles in a pulse tube refrigerator

Ling Chen [a], Yu Zhang [a,*], Ercang Luo [b], Teng Li [a], Xiaolin Wei [a]

[a] Key Laboratory of Environmental Mechanics, The Institute of Mechanics, Chinese Academy of Sciences, Beijing 100190, China
[b] Key Laboratory of Cryogenics, The Technical Institute of Physics and Chemistry, Chinese Academy of Sciences, Beijing 100190, China

ARTICLE INFO

Article history:
Received 7 June 2010
Received in revised form 18 August 2010
Accepted 26 August 2010

Keywords:
Pulse tube refrigerator
CFD
Thermodynamic cycles

ABSTRACT

The objectives of this paper are to study the thermodynamic cycles in an inertance tube pulse tube refrigerator (ITPTR) by means of CFD method. The simulation results show that gas parcels working in different parts of ITPTR undergo different thermodynamic cycles. The net effects of those thermodynamic cycles are pumping heat from the low temperature part to the high temperature part of the system. The simulation results also show that under different frequencies of piston movement, the gas parcels working in the same part of the system will undergo the same type of thermodynamic cycles. The simulated thermal cycles are compared with those thermodynamic analysis results from a reference. Comparisons show that both CFD simulations and theoretical analysis predict the same type of thermal cycles at the same location. However, only CFD simulation can give the quantitative results, while the thermodynamic analysis is still remaining in quality.

1. Introduction

Pulse tube refrigerator (PTR) has many advantages over conventional refrigerators, such as no moving part, low cost, high reliability and less mechanical vibration. Therefore, the PTR is recognized as one of the most promising refrigerators in the future. Since the invention of the basic pulse tube refrigerator (BPTR) in the early 1960s [1], pulse tube refrigerator has experienced several significant structural improvements including the orifice pulse tube refrigerator (OPTR) [2], the double inlet pulse tube refrigerator (DIPTR) [3], the multi-stage pulse tube refrigerator [4] and most recently the inertance tube pulse tube refrigerator (ITPTR) [5]. All of these improvements have led to the technical progress of the PTR, and so far the lowest temperature attained by the pulse tube refrigerator has already reached about 1.3 K [6].

However, till now, the mechanism of PTR has still not yet been fully understood. Several theories have been developed to explain the refrigeration mechanism of PTRs since their invention. Gifford and Longsworth first explained the refrigeration effect in BPTR by a process named surface heat pumping [7], which is determined by both the thermal interactions between the wall of the BPTR and the properties of the working gas; however, this theory is only suitable for PTRs operating under low frequencies. Peter and Radebaugh [8] assumed that phase shift between pressure and the mass flow rate is the major mechanism for heat transfer in PTRs. In 1990s, Liang et al. [9] proposed thermodynamic non-symmetry effect to illustrate the refrigeration in PTRs. This theory points out that when gas flows through a tube half filled with porous material, it will experience strong non-symmetric heat exchange and consequently generate refrigeration. Besides those discussions, thermo-acoustic effect is also introduced to explain the mechanism of PTRs. However, all of these theories have their own limitations and cannot explain the mechanism of the PTRs adequately.

The theories mentioned above fail to give detail information of thermodynamic processes of the working gas in a cycle, which must be important for understanding the mechanism of PTRs. The thermodynamic processes of the working gas in PTR are very different from those described in classical thermodynamic cycles such as an ideal Stirling cycle, in which every portion of the gas is assumed to undergo the exact same thermodynamic cycle. In PTR each small portion of the working gas, viz. a gas parcel, oscillates only in a small part, and the thermal cycles at different parts should be also different [10]. In 1997, Liang [10] proposed a sinusoidal model to analyze the thermodynamic processes of gas parcels oscillating in a regenerator. In his analysis, results show that each gas parcel in the regenerator works as either a heat engine or a refrigerator. But Liang did not attain the transient temperature of the gas parcel and the obtained function of the regenerator is questionable. In 2004, a further theoretical study was conducted by Luo [11] to investigate the thermodynamic cycles in the regenerator. That theory is named as meso-scope thermodynamic theory. With some assumptions and thorough mathematical computation, the thermodynamic cycles of these characteristic gas parcels were attained. However, in Luo's analysis some assumptions such as the working gas has no viscosity, the phase

* Corresponding author. Tel.: +86 10 82544231; fax: +86 10 62561284.
E-mail address: zhangyu@imech.ac.cn (Y. Zhang).

0011-2275/$ - see front matter © 2010 Elsevier Ltd. All rights reserved.
doi:10.1016/j.cryogenics.2010.08.004

Nomenclature

X	piston displacement (m)
X_a	piston displacement amplitude (m)
f	operating frequency (Hz)
t	time (s)
v	intrinsic velocity (m/s)
E	energy (J/kg)
p	pressure (bar)
υ	specific volume (m^3/kg)
T	temperature (K)
s	specific entropy (J/kg K)
k	thermal conductivity (W/m K)
h	enthalpy (J/kg)
C_2	initial resistance factor (m^{-1})
C_p	specific heat (J/kg K)
R	gas constant (J/kg K)

Greek letters

ω	angular frequency
γ	porosity
ρ	density (kg/m^3)
α	permeability
μ	viscosity (kg/m s)
$\vec{\tau}$	stress tensors (N/m^2)

Subscripts

f	fluid
r	radial coordinate
s	solid
x	axial coordinate
ref	reference

shift between fluctuated pressures and flow rates is keeping uniform everywhere, are not reasonable. Furthermore, those analyses are still qualitative, but have no quantitative meanings.

In this paper, two-dimensional axi-symmetric CFD simulations are conducted to analyze the thermodynamic processes in ITPTR. Instead of assumptions, CFD method directly calculates the gas velocity, the gas temperature, the gas pressure and the phase shift of different variables at different locations. After CFD calculations, summarizing the obtained results in Lagrangian's view, the quantitative results of thermodynamic cycles will come out.

2. Simulation model

A two-dimensional, axi-symmetric schematic of the ITPTR system is shown in Fig. 1. The sizes of all parts of the system are listed in Table 1. The details of the simulated system can be found in the publication of Cha et al. [12].

A commercial CFD code Fluent [14] is applied in this simulation. The amount of computational cells reaches 4600. The piston movement is described as

$$X = X_a \sin(\omega t) \tag{1}$$

where X_a = 4.511 mm is the amplitude, $\omega = 2\pi f$ is the angular velocity and f is the operating frequency. A User Define Function (UDF) is written to track and guide the movement of the piston.

The mass, momentum, and energy equations solved by Fluent for the working gas are [12,14]

$$\frac{\partial \rho_f}{\partial t} + \frac{1}{r}\frac{\partial}{\partial r}(r\rho_f v_r) + \frac{\partial}{\partial x}(\rho_f v_x) = 0 \tag{2}$$

$$\frac{\partial}{\partial t}(\rho_f \vec{v}) + \nabla\cdot(\rho_f \vec{v}\vec{v}) = -\nabla p + \nabla\cdot(\vec{\tau}) \tag{3}$$

Table 1
Dimensions of the ITPTR.

Components	Diameter (mm)	Length (mm)
Compressor	19.08	7.5
Transfer line	3.1	101
WHX1	8	20
Regenerator	8	58
CHX	6	5.7
Pulse tube	5	60
WHX2	8	10
Inertance tube	0.85	684
Reservoir	26	130

$$\frac{\partial}{\partial t}(\rho_f E) + \nabla\cdot(\vec{v}(\rho_f E + p)) = \nabla\cdot\left[k_f \nabla T + \left(\vec{\tau}\cdot\vec{v}\right)\right] \tag{4}$$

where

$$E = h - \frac{p}{\rho} + \frac{v^2}{2} \tag{5}$$

The mass, momentum and energy equations for the porous media are as follows:

$$\frac{\partial}{\partial t}(\gamma\rho_f) + \frac{1}{r}\frac{\partial}{\partial r}(\gamma r\rho_f v_r) + \frac{\partial}{\partial x}(\gamma\rho_f v_x) = 0 \tag{6}$$

$$\frac{\partial}{\partial t}(\gamma\rho_f \vec{v}) + \nabla\cdot(\gamma\rho_f \vec{v}\vec{v}) = -\gamma\nabla p + \nabla\cdot\left(\gamma\vec{\tau}\right) - \left(\frac{\mu}{\alpha}\vec{v} + C_2\frac{1}{2}\rho_f|\vec{v}|\vec{v}\right) \tag{7}$$

$$\frac{\partial}{\partial t}[\gamma\rho_f E_f + (1-\gamma)\rho_s E_s] + \nabla\cdot[\vec{v}(\rho_f E_f + p)] = \nabla\cdot\left[(\gamma k_f + (1-\gamma)k_s)\nabla T + \left(\gamma\vec{\tau}\cdot\vec{v}\right)\right] \tag{8}$$

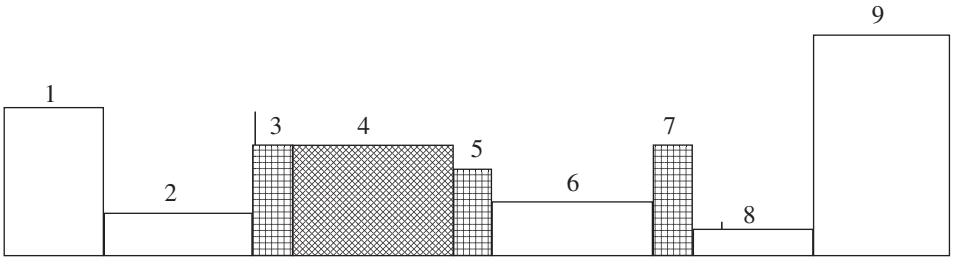

Fig. 1. Schematic of the physical model of ITPTR: (1) compressor, (2) transfer line, (3) after cooler (WHX1), (4) regenerator, (5) cold end heat exchanger (CHX), (6) pulse tube, (7) hot end heat exchanger (WHX2), (8) inertance tube, and (9) reservoir.

where γ is porosity of the porous media, α is the permeability and C_2 is the inertial resistance factor. In simulation, $\gamma = 0.69$, $\alpha = 1.06 \times 10^{-10}$ m^2, and $C_2 = 7.609 \times 10^4$ m^{-1}.

In this simulation, the working gas is helium, which is modeled as a compressible ideal gas. Its viscosity is set to be temperature-dependent. The walls of WHX1 and WHX2 are maintained at 300 K while all the other system walls are assumed to be adiabatic. The initial temperature of the system is 300 K. Each period of the piston movement is divided into 50 time steps. The convergence tolerance criterion for energy equations is 1×10^{-6} and that for other equations is 0.001. Running one case by a computer with 2.2 GHz processor and 2.0 GB RAM till steady state takes a month or even more.

In order to study the thermodynamic cycles of the working gas in refrigerator, some characteristic gas parcels are chosen. These gas parcels are: gas parcel oscillating in after cooler (WHX1) and regenerator; gas parcel oscillating entirely in regenerator; and gas parcel oscillating in regenerator and CHX. The gas parcels chosen are located on the axis where the radial velocities of the gas parcels are far smaller than the axial velocities, so that the influences of the radial velocities of the gas parcels can be neglected. A schematic of gas parcels chosen for thermodynamic analysis is shown in Fig. 2.

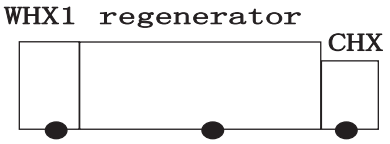

Fig. 2. Schematics of gas parcels for thermodynamic analysis.

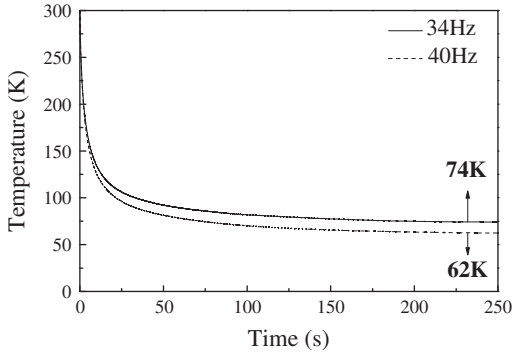

Fig. 3. Variations of cycle-average temperature of CHX wall surface for simulation cases.

Thermodynamic cycle of a gas parcel can be drawn on pressure-specific volume (p–υ) diagram and temperature-specific entropy (T–s) diagram. The specific entropy change from the reference state of a gas parcel can be calculated as follows:

$$s = C_p \ln\left(\frac{T}{T_{\text{ref}}}\right) + R \ln\left(\frac{p_{\text{ref}}}{p}\right) \tag{9}$$

where $T_{\text{ref}} = 288.15$ K, $p_{\text{ref}} = 1.01325$ bar.

An additional Lagrangian method is used as a post-process to track the movement of a gas parcel to get its pressure p, specific volume υ, temperature T and axial velocity v at different positions in a thermocycle. At time t, the pressure, specific volume and axial velocity of a chosen gas parcel are p_t, υ_t and v_t. T_t and s_t of the gas parcel can be obtained from ideal gas equation and Eq. (9). Assuming that the axial velocity of the gas parcel is keeping constant during a time step Δt (if Δt is small enough), therefore the gas parcel will move to a new certain position at time $t + \Delta t$. If the new position is not located in a grid point, $p_{t+\Delta t}$, $\upsilon_{t+\Delta t}$ and $v_{t+\Delta t}$ of the gas parcel are calculated by linear interpolation of those parameters at two adjacent grids. Again $T_{t+\Delta t}$ and $s_{t+\Delta t}$ of the gas parcel can be obtained from ideal gas equation and Eq. (9). After 50 time steps calculations, the gas parcel will return to its original position. Therefore thermodynamic cycles of the gas parcel can be obtained.

3. Results and discussion

3.1. Refrigeration performance

In this paper, the pulse tube refrigerator system has been simulated under two different operating frequencies, viz. the frequency of piston movement: 34 Hz and 40 Hz. The frequency 34 Hz was in fact used in Havey's experiment [13]. The variations

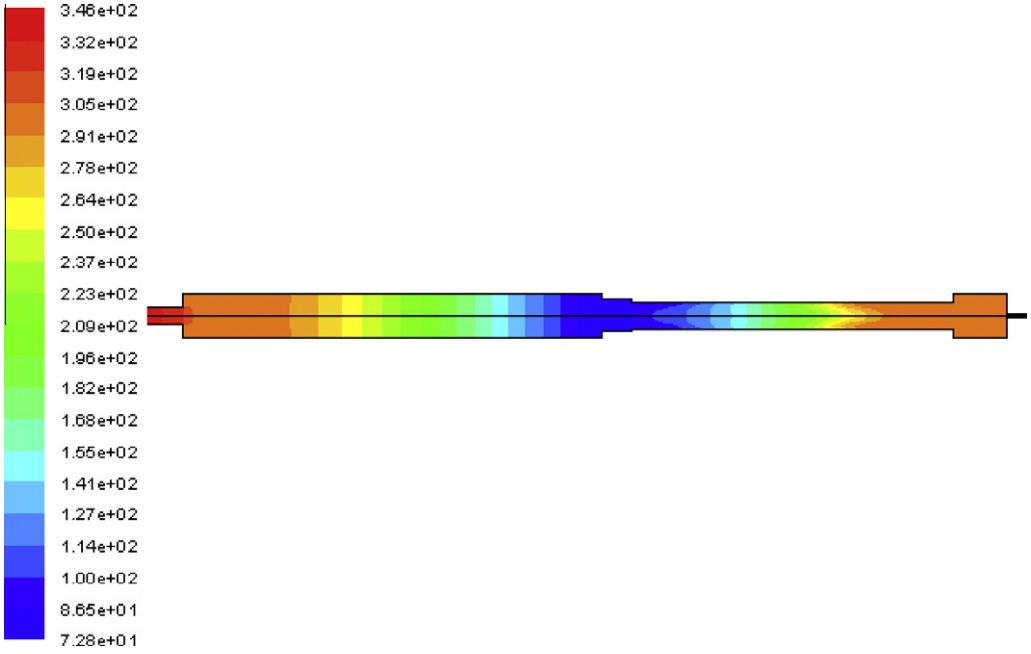

Fig. 4. Temperature contour for 34 Hz frequency case.

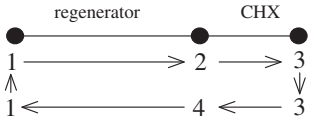

Fig. 5. A schematic of the working processes of a gas parcel oscillating in regenerator and CHX in a cycle.

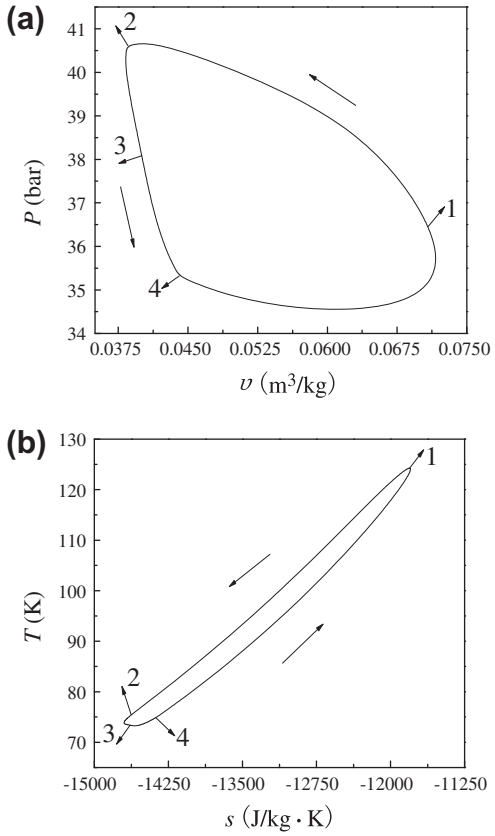

Fig. 6. (a) p–υ Diagram of the gas parcel oscillating in regenerator and CHX for the 34 Hz frequency case. (b) T–s diagram of the gas parcel.

of cycle-average temperature of CHX wall surface are shown in Fig. 3 for the two cases. For 34 Hz frequency case, the simulated steady cycle-average temperature of CHX wall surface is 74 K, which is lower than the experimental result 87 K. The error between the simulation and experiment may be induced by the ideal gas assumption, the laminar flow assumption, or without wall thickness consideration. The 40 Hz frequency case has better performance than the 34 Hz frequency case, in which the simulated steady cycle-average CHX wall surface temperature is 62 K.

Snapshot of the temperature contour along axial direction for 34 frequency case is shown in Fig. 4. It can be seen that the lowest temperature of the pulse tube refrigerator is mainly appearing in the CHX part.

3.2. Thermodynamic cycles of gas parcels

3.2.1. Thermodynamic cycle of a gas parcel oscillating in regenerator and CHX

As discussed above, the lowest temperature is appearing in CHX part. However, the CHX is very short in length, and it is hard to find a gas parcel that only oscillates inner the CHX, so the gas parcel chosen is oscillating in both the regenerator and the CHX. As shown in Fig. 5, the cycle of the gas parcel is characterized by four points: point 1 is the leftmost position of the gas parcel in regenerator, point 3 is the rightmost position of the gas parcel in CHX (point 3 is in fact the outlet position of the CHX), points 2 and 4 correspond to the entrance position of the CHX.

The p–υ and T–s diagrams of the gas parcel oscillating in regenerator and CHX for the 34 Hz frequency case are shown in Fig. 6a and b. The work and the heat transfer of the gas parcel during each cycle are listed in Tables 2 and 3. According to Fig. 6, the net effect of the cycle is consuming work and releasing heat. From point 1 to point 2, the gas parcel experiences a compression process through regenerator. During processes 1–2, the gas parcel releases heat, and the amount of heat out is larger than the amount of work in, so the temperature of the gas parcel decreases. During processes 2–3 within CHX, the gas parcel produces work but also releases heat, the temperature of the gas parcel further decreases. During processes 3–4, the gas parcel produces work and absorbs heat, and the work produced by the gas parcel is lower than the heat absorbed by the gas parcel, so the temperature of the gas parcel increases. During processes 4–1, the gas parcel continues to produce work and absorb heat, and also the amount of work out is lower than the amount of heat in, as a result the temperature of the gas parcel further increases to the original status. Moreover, it can be seen that the amount of heat in during processes 3–4 is larger than the amount of heat out during processes 2–3 within CHX. Thus the net effect of the gas parcel oscillating within CHX is absorbing heat and producing work. This explains why the lowest temperature is appearing in CHX. Noted that during the processes 1–2 and 4–1 within the regenerator, the net effect of the gas parcel is consuming work and releasing heat. And the amount of heat released by the gas parcel within regenerator is larger than the amount of heat absorbed within CHX. The difference exactly equals to the net work of the cycle required. So in a cycle, the gas parcel absorbs heat in CHX, consumes work and releases heat in regenerator like a heat pump.

All the illustrations above are for the refrigerator operating at 34 Hz frequency. The thermodynamic cycle of the gas parcel oscillating in regenerator and CHX for the 40 Hz frequency case is also shown in Fig. 7. Compared Figs. 6 and 7, it can be seen that

Table 2
Work of the gas parcel in each process and in a cycle.

W_{1-2} (J/kg)	W_{2-3} (J/kg)	W_{3-4} (J/kg)	W_{4-1} (J/kg)	$W_{1-2}+W_{4-1}$ (J/kg)	$W_{2-3}+W_{3-4}$ (J/kg)	W_{12341} (J/kg)
−127327.2	5729.9	14661.3	93370.3	−33956.9	20391.2	−13565.7

Table 3
Heat transfer of the gas parcel in each process and in a cycle.

q_{1-2} (J/kg)	q_{2-3} (J/kg)	q_{3-4} (J/kg)	q_{4-1} (J/kg)	$q_{1-2}+q_{4-1}$ (J/kg)	$q_{2-3}+q_{3-4}$ (J/kg)	q_{1234} (J/kg)
−280072.6	−382.6	19284.9	247604.6	−32468	18902.3	−13565.7

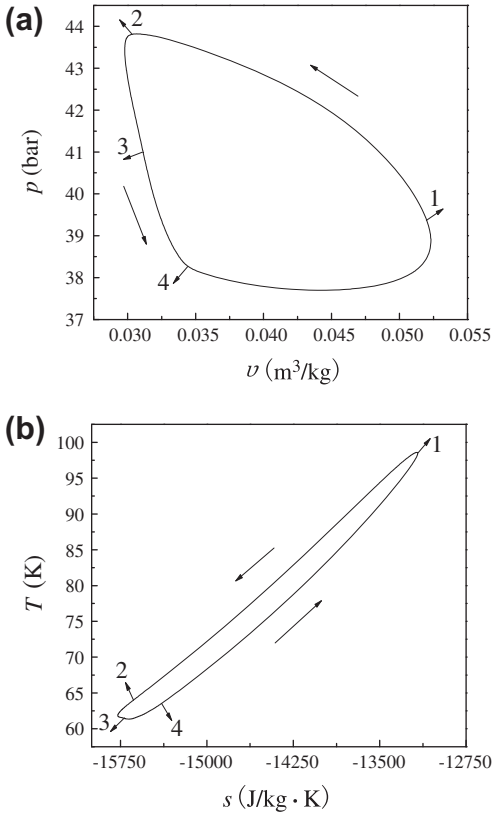

Fig. 7. (a) p–υ Diagram of the gas parcel oscillating in regenerator and CHX for the 40 Hz frequency case. (b) T–s diagram of the gas parcel.

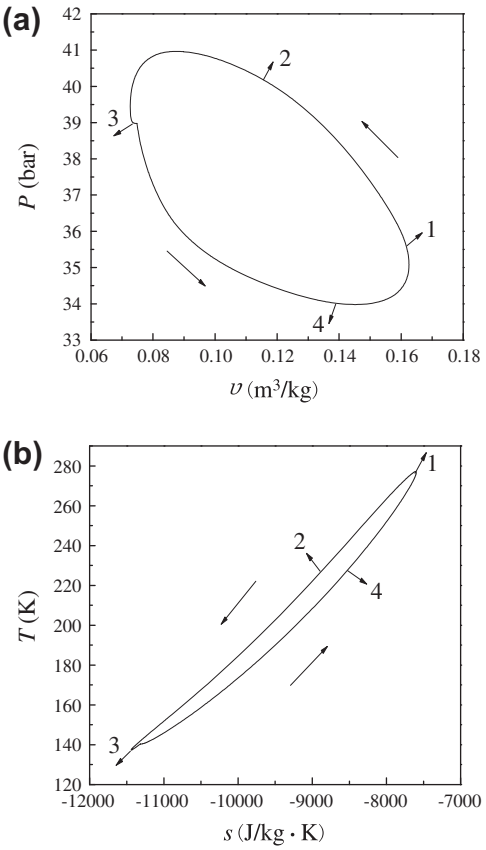

Fig. 9. (a) p–υ Diagram of the gas parcel oscillating in regenerator for the 34 Hz frequency case. (b) T–s diagram of the gas parcel.

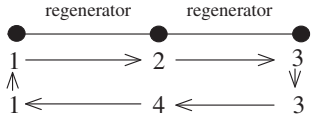

Fig. 8. A schematic of the working processes of a gas parcel oscillating in regenerator in a cycle.

thermodynamic cycle of the gas parcel oscillating in regenerator and CHX for the 40 Hz frequency case are very similar to that for the 34 Hz frequency case. The results indicate that at the same location the working gases of different frequencies undergo the same type of thermodynamic cycles.

3.2.2. Thermodynamic cycles of gas parcels oscillating in regenerator

From Fig. 8, it can be observed that the cycle of a gas parcel oscillating in regenerator is characterized by four points: point 1 is the leftmost position, point 3 is the rightmost position, points 2 and 4 are the central position of the regenerator.

Fig. 9a shows the p–υ diagram of the gas parcel oscillating in regenerator for the 34 Hz frequency case, and Fig. 9b shows the T–s diagram of the gas parcel. The work and heat transfer of the gas parcel are listed in Tables 4 and 5.

Clearly, the gas parcel oscillating in regenerator also undergoes a cycle consuming work and releasing heat. During the processes 1–2 and 2–3, the gas parcel consumes work and releases heat, while during the processes 3–4 and 4–1, the gas parcel produces work and absorbs heat. During processes 2–3–4, the net effect of the gas parcel is absorbing heat and producing work in the low temperature part. While during the processes 4–1–2, the net effect of the gas parcel is consuming work and releasing heat in the high temperature part. And again the amount of heat released in the high temperature part of the regenerator is larger than the heat absorbed in the low temperature part of the regenerator, and the difference equals to the

Table 4
Work of the gas parcel in each process and in a cycle.

W_{1-2} (J/kg)	W_{2-3} (J/kg)	W_{3-4} (J/kg)	W_{4-1} (J/kg)	$W_{1-2} + W_{4-1}$ (J/kg)	$W_{2-3} + W_{3-4}$ (J/kg)	W_{12341} (J/kg)
−184788.7	−155759.5	222361.8	78563.1	−106225.6	66602.3	−39623.3

Table 5
Heat transfer of the gas parcel in each process and in a cycle.

q_{1-2} (J/kg)	q_{2-3} (J/kg)	q_{3-4} (J/kg)	q_{4-1} (J/kg)	$q_{1-2} + q_{4-1}$ (J/kg)	$q_{2-3} + q_{3-4}$ (J/kg)	q_{1234} (J/kg)
−361683.4	−405817.1	493270.5	234606.7	−127076.7	87453.4	−39623.3

net work of the gas parcel in a cycle. So the gas parcel also consumes work and pumps heat from the right low temperature part to the left high temperature part of the regenerator. The way of heat transfer within the regenerator is very similar with that between CHX and regenerator. It should be noted that thermodynamic cycle of the gas parcel oscillating in regenerator of 40 Hz frequency case is also very similar with that of the 34 Hz frequency case.

Fig. 10 is the thermodynamic cycle of a gas parcel oscillating in a regenerator attained by Luo [11] from pure thermodynamic analysis. The four points characterized the thermodynamic cycles in Fig. 10a and b have the same meaning with those in Figs. 8–10. It can be seen that thermodynamic cycle of the gas parcel oscillating in regenerator is quite similar between simulation and theoretical analysis. But the later one is only qualitative.

Fig. 11a and b shows the p–υ diagrams and T–s diagrams of four adjacent gas parcels oscillating entirely in regenerator. Gas parcel 1 lies in the rightmost while gas parcel 4 lies in the leftmost. From Fig. 11, it can be seen that each gas parcel in regenerator undergoes the same type of thermodynamic cycle but at different temperatures. And all of the gas parcels in regenerator work together to pump heat from the low temperature part to the high temperature part of the regenerator.

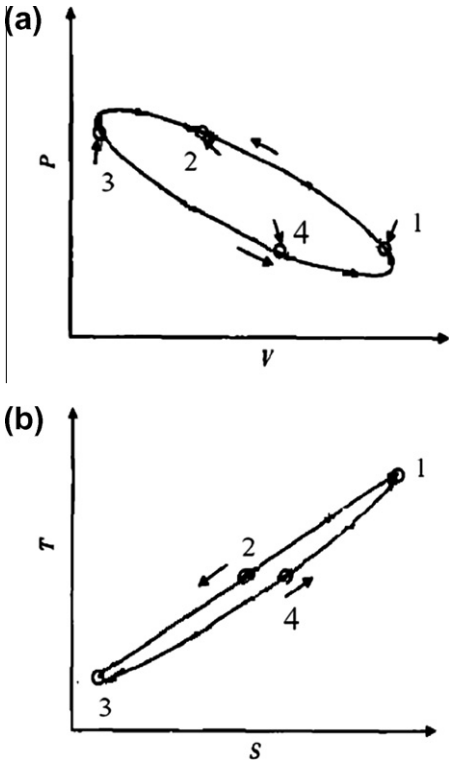

Fig. 10. (a) p–υ Diagram of the gas parcel oscillating in regenerator theoretical attained by Luo [11]. (b) T–s diagram of the gas parcel.

3.2.3. Thermodynamic cycle of a gas parcel oscillating in WHX1 and regenerator

As shown in Fig. 12, the cycle of the gas parcel oscillating in WHX1 and regenerator is also characterized by four points: point

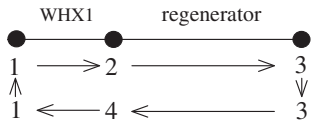

Fig. 12. A schematic of the working processes of a gas parcel oscillating in WHX1 and regenerator in a cycle.

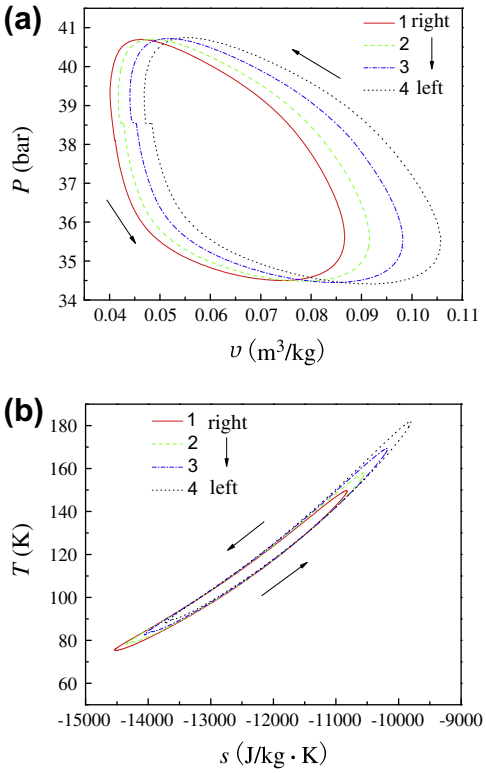

Fig. 11. (a) p–υ Diagrams of the gas parcels oscillating in regenerator for 34 Hz frequency case. (b) T–s diagrams of those gas parcels.

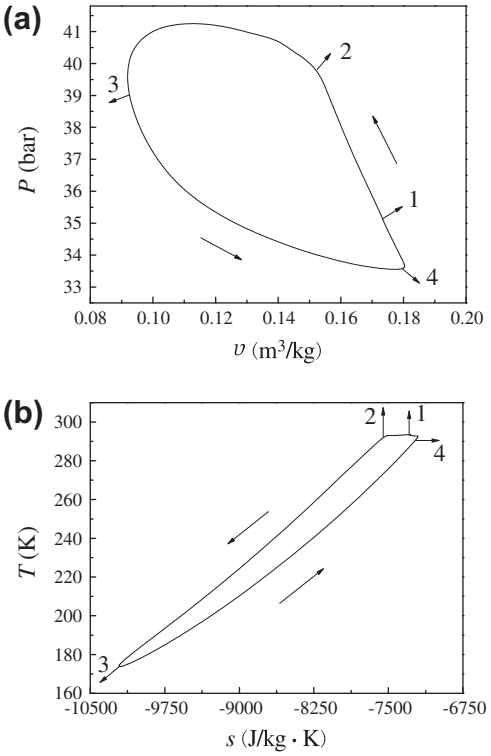

Fig. 13. (a) p–υ Diagram of the gas parcel oscillating in WHX1 and regenerator for the 34 Hz frequency case. (b) T–s diagram of the gas parcel.

Table 6
Work of the gas parcel in each process and in a cycle.

W_{1-2} (J/kg)	W_{2-3} (J/kg)	W_{3-4} (J/kg)	W_{4-1} (J/kg)	$W_{1-2} + W_{4-1}$ (J/kg)	$W_{2-3} + W_{3-4}$ (J/kg)	W_{12341} (J/kg)
−77670.8	−245901.9	299695.8	−16603.9	−94274.7	53793.9	−40480.8

Table 7
Heat transfer of the gas parcel in each process and in a cycle.

q_{1-2} (J/kg)	q_{2-3} (J/kg)	q_{3-4} (J/kg)	q_{4-1} (J/kg)	$q_{1-2} + q_{4-1}$ (J/kg)	$q_{2-3} + q_{3-4}$ (J/kg)	q_{1234} (J/kg)
−81013.3	−615532.2	677157.3	−21092.6	−102105.9	61625.1	−40480.8

1 is the leftmost position in WHX1, point 3 is the rightmost position in regenerator, and points 2 and 4 locate on the entrance position of the regenerator. The p–υ diagram and T–s diagram of the gas parcel are shown in Fig. 13a and b. The work and heat transfer of the gas parcel are listed in Tables 6 and 7.

It can be seen that when the gas parcel oscillates in regenerator part, it absorbs heat and produces work, and when it oscillates in WHX1 part, it consumes work and releases heat. Over all, the gas parcel oscillating in WHX1 and regenerator also consumes work and pumps heat from the low temperature part (right in regenerator) to the high temperature part (left in WHX1). The heat released in WHX1 by the gas parcel will be ultimately conveyed to the WHX1 wall surface, where the temperature is maintaining at 300 K. Again, thermodynamic cycle of the gas parcel oscillating in WHX1 and regenerator for 40 Hz frequency is similar to that for 34 Hz frequency case.

4. Conclusions

In this paper an inertance tube pulse tube refrigerator is simulated by a two-dimensional axial-symmetric CFD model. The simulation results are summarized in Lagrangian's view and the thermodynamic cycles of gas parcels are obtained. Results show that different gas parcels undergo thermodynamic cycles at different temperatures. These gas parcels convey heat from the low temperature part to the high temperature part of the system. Finally, the heat will be released from the after cooler wall surface, where the temperature is keep at 300 K. Results of different operating frequency cases indicate that the working gas parcels at the same part of the system but under different working conditions might undergo the same type of thermodynamic cycles. The thermodynamic cycles in the regenerator are summarized from CFD calculations, and are compared with the thermodynamic analysis result from a reference. Comparison shows that both CFD simulation and theoretical analysis can predict the similar thermodynamic cycles, but only CFD simulation gives the quantitative results.

Acknowledgement

This work is supported by the National Science Foundation of China under Contract No. 50890182.

References

[1] Gifford W, Longsworth R. Pulse tube refrigeration. Trans ASME, J Eng Ind (Ser B) 1964;86:264–8.
[2] Mikulin EA, Tarasov AA, Shkrebyonock MP. Low-temperature expansion pulse tubes. Adv Cryo Eng 1984;29:629–37.
[3] Zhu S, Wu P, Chen Z. A single stage double inlet pulse tube refrigerator capable of reaching 42 K. In: ICEC 13 proc cryogenics, Beijing, vol. 30; 1990. p. 256–61.
[4] Cai J, Wang J, Zhou Y. Experimental analysis of double-inlet principle in pulse tube refrigerator. Cryogenics 1993;33:522–5.
[5] Kanao K, Watanabe N, Kanazawa Y. A miniature pulse tube refrigerator for temperature below 100 K. Cryogenics 1994;34(suppl. 1):167–70.
[6] Jiang N. A 3He pulse tube cooler operating down to 1.3 K. Cryogenics 2004;44(11):809–16.
[7] Gifford W, Longsworth R. Surface heat pumping. Adv Cryo Eng 1966;11:171–81.
[8] Peter S, Radebaugh R. Development and experimental test of an analysis model of the orifice pulse tube refrigerator. Adv Cryo Eng 1987;33:851–9.
[9] Liang J, Ravex A, Rolland P. Study on pulse tube refrigeration part 1: thermodynamic non-symmetry effect. Cryogenics 1996;36(2):87–93.
[10] Liang J. Thermodynamic cycles in oscillating flow regenerators. J Appl Phys 1997;82(9):4159–63.
[11] Luo E, Dai W, Wu Z, et al. Meso-scope thermodynamic theory for cyclic flow engines. Cryogenics 2004;1:1–11 [in Chinese].
[12] Cha J, Ghiaasiaan S, Desai P, et al. Multi-dimensional flow effects in pulse tube refrigerators. Cryogenics 2006;46:658–65.
[13] Harvey J. Oscillatory compressible flow and heat transfer in porous media application to cryocooler. PhD thesis. Georgia Institute of Technology, Atlanta; 2003.
[14] Fluent INC. Fluent 6 user manual. Fluent INC; 2003.